Supporting Information for:

Self-organized Au Nanoarrays on Vertical Graphenes: an Advanced Three-dimensional Sensing Platform

Amanda E. Rider,[1,2,†], Shailesh Kumar[1,†], Scott A. Furman[1], Kostya (Ken) Ostrikov[1,2,]*

[1] Plasma Nanoscience Centre Australia (PNCA), CSIRO Materials Science and Engineering, P.O. Box 218, Lindfield, New South Wales 2070, Australia.

[2] Complex Systems, School of Physics, The University of Sydney, NSW 2006, Australia.

[†]Authors who made equal contributions to this article

* Author to whom correspondence should be addressed: Kostya.Ostrikov@csiro.au

Contents:

(1) Experimental Set-up and details

(2) Elemental, Morphological and structural analysis

(3) Discussion of Au nanoparticle formation and reasons for quasi-linear NP self-organization

(4) Calculations of typical surface coverages and 'bookshelf' coverage

(5) Further discussion of the Raman spectra for Au-VGNS prior to 4-ATP immersion

(6) References for Supporting Information

(1) Experimental Set-Up and details

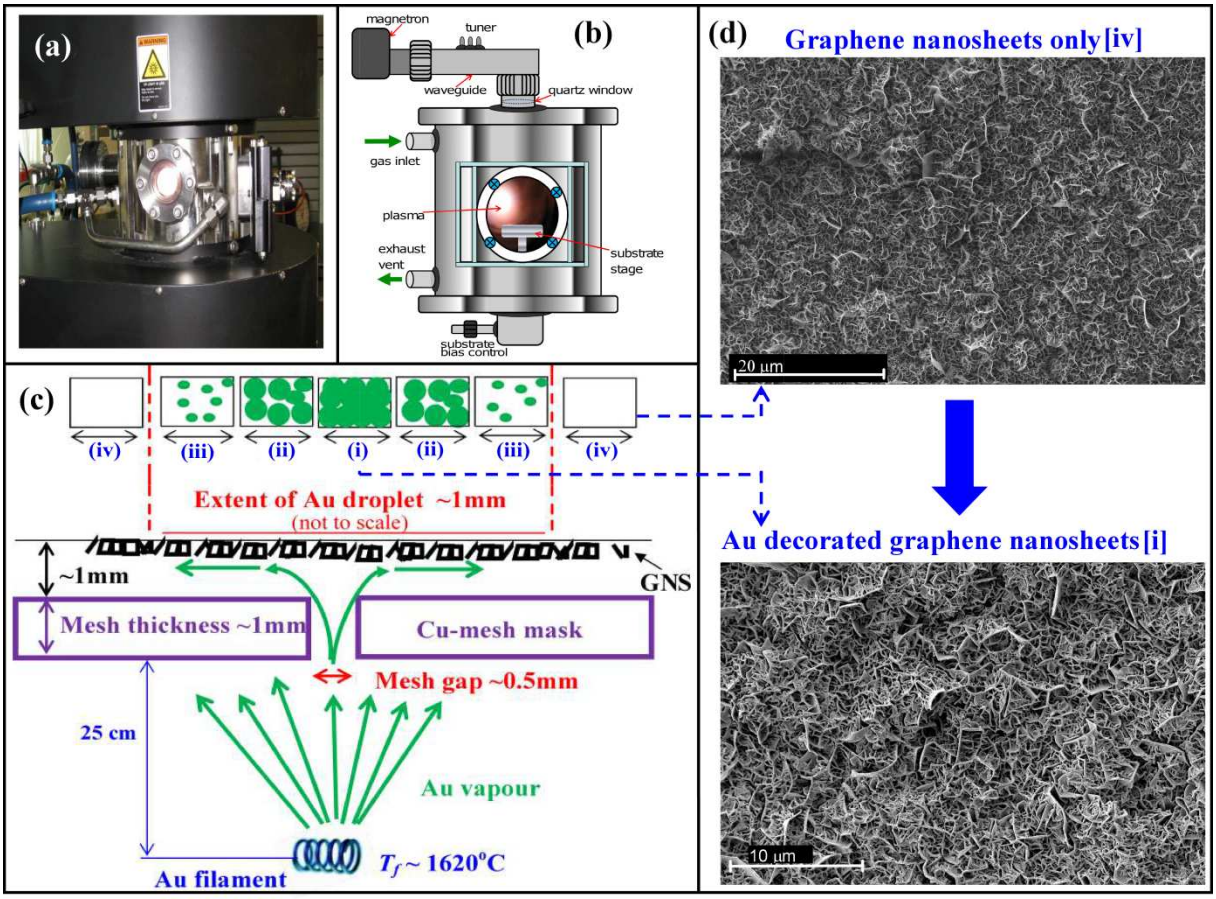

Fig. S1. (Microwave PECVD reactor used in GNS synthesis; (b) Schematic of the microwave PECVD reactor; (c) Schematic for hot-filament plasma-assisted thermal evaporation of Au NPs on the GNS sample. Here, (iv) indicates the part of the sample where no Au is present, only GNS, moving radially outwards (iii) indicates smaller, sparse patterns of Au NPs, (ii) is dense pattern of large Au NPs and (i) is an almost continuous Au film located at the center of the mesh hole. Scanning electron micrographs of typical (i) and (iv) patterns are provided in (d))

Experimental Details

Growth of Au-VGNS: The VGNS were deposited via plasma enhanced chemical vapour deposition on a Si(100) substrate. The substrate was pre-treated prior to the deposition through exposure to a N_2 plasma for 5 min (N_2 inlet was 50 sccm, microwave power was 500 W and chamber pressure was 7 Torr) with the substrate temperature reaching approximately 400 ^{o}C. This was followed by deposition for 10 min using process parameters: CH_4 /N_2 gas inlet ratio of 1:1, input power of 750 W and chamber pressure of 10 Torr. At the end of the deposition process the substrate temperature was measured to be ~ 800 ^{o}C.

Thermal evaporation of gold onto the VGNS was carried out at room temperature using process parameters: filament temperature ~ 1620 ^{o}C, distance between the sample and the filament ~25 cm, diameter of mesh between the sample and the filament of 0.5 mm, thickness of mesh ~ 1 mm and distance between mesh and sample ~1 mm and a chamber pressure of 2.0×10^{-6} Torr.

Characterization and Analysis: SEMs were taken using a Zeiss Ultra Plus Scanning Electron Microscope set at 4 kV. A Renishaw inVia Raman Microscope (with a 633 nm laser excitation source, room temperature excitation) was used to acquire micro-Raman spectra from the observably highest concentration of Au nanoparticles through to VGNS only. HR-TEMs were taken using a JEOL 3000F Transmission Electron Microscope using a 300 kV accelerating voltage.

Test of sensing performance: The Au-VGNS arrays were immersed in 10^{-2}M 4-ATP (prepared from solid 4-ATP, 97%, Aldrich, dissolved in ethanol) for 6 hours. They were removed and allowed to dry overnight in air. SERS spectra were taken by a Renishaw inVia

confocal Raman microscope (50x objective lens, 633 nm HeNe laser operating at 1% laser power, an exposure time of 10 s and 3 accumulations). The colloidal Au NPs (reference samples) drop-dried on SiO_2/Si(100) [0.05mg mL^{-1} of 3-4 nm Au NPs stabilised in tannic acid, in aqueous solution, used as received from PlasmaChem, Germany] were immersed in ~10^{-2}M 4-ATP for 5 ½ hours and dried in air; SERS spectra were taken using same settings as above, but 1 accumulation only.

N. B. For additional information on various approaches to 4-ATP tests in the literature, we refer the interested reader to the following papers [J. Ye *et al*., *Appl. Phys. Lett*. **97**, 163106 (2010); Junwei Zheng *et al*., *Langmuir* **19**, 632–636 (2003); Li Wang *et al*, *Colloids and Surfaces A: Physicochem. Eng. Aspects* **312**, 148–153 (2008); Y. Wang *et al*., *J. Chem. Phys.* **124**, 074709 (2006)]

(2) Elemental, Morphological and structural analysis:

Compositional mapping was undertaken using a Zeiss Ultra Plus Scanning Electron Microscope in combination with with a Bruker XFlash 4010 EDS detector where the electron gun was set at 20 kV. An X-ray diffraction (XRD) spectrum was collected using a Phillips Xpert Pro MPD (Gonio PW3050/60) with a Cu tube.

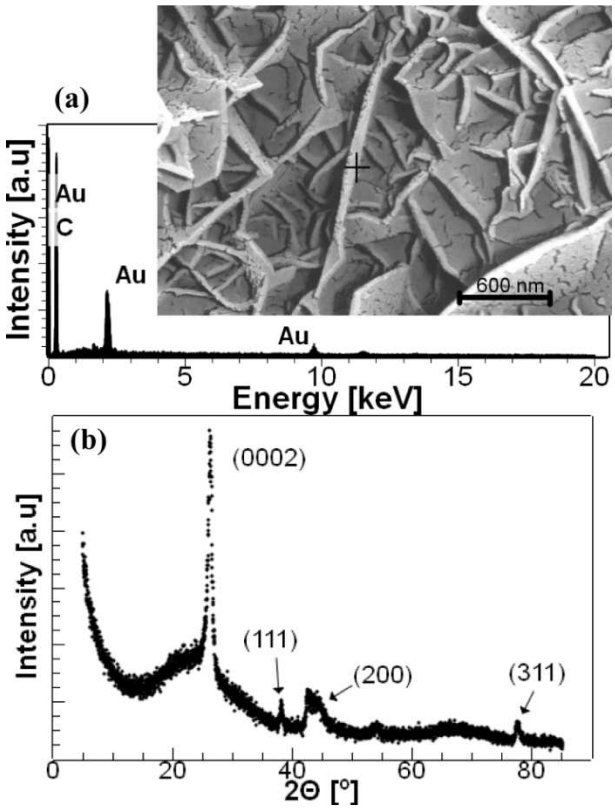

Fig. S2 presents evidence of the presence of both C and Au in the sample via energy dispersive spectroscopy (EDS). A point spectra showing the presence of both C and Au is provided in Fig S2(a). An X-ray diffraction (XRD) spectrum is provided in Fig S2(b), the peak at $2\theta \sim 26^{o}$ is indicative of graphitic carbon (0002), the peaks at ~38.2^{o}, ~44^{o} and ~77.4^{o} indicate Au(111), Au(200) and Au(311) phases, respectively.[1,2]

Figure S3 below shows clear evidence of particle-like distribution of Au on C.

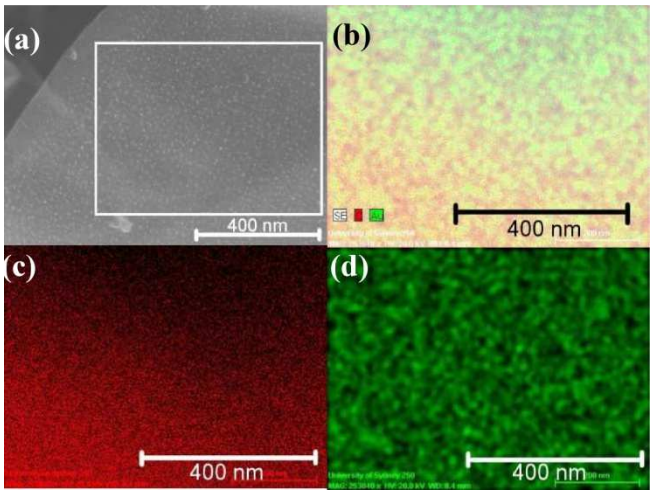

Fig. S3 EDS data for Au NP on GNS sample: (a) SEM with acquisition area marked with a white square, (b) compositional map combined, (c) C only [red], (d) Au only [green].

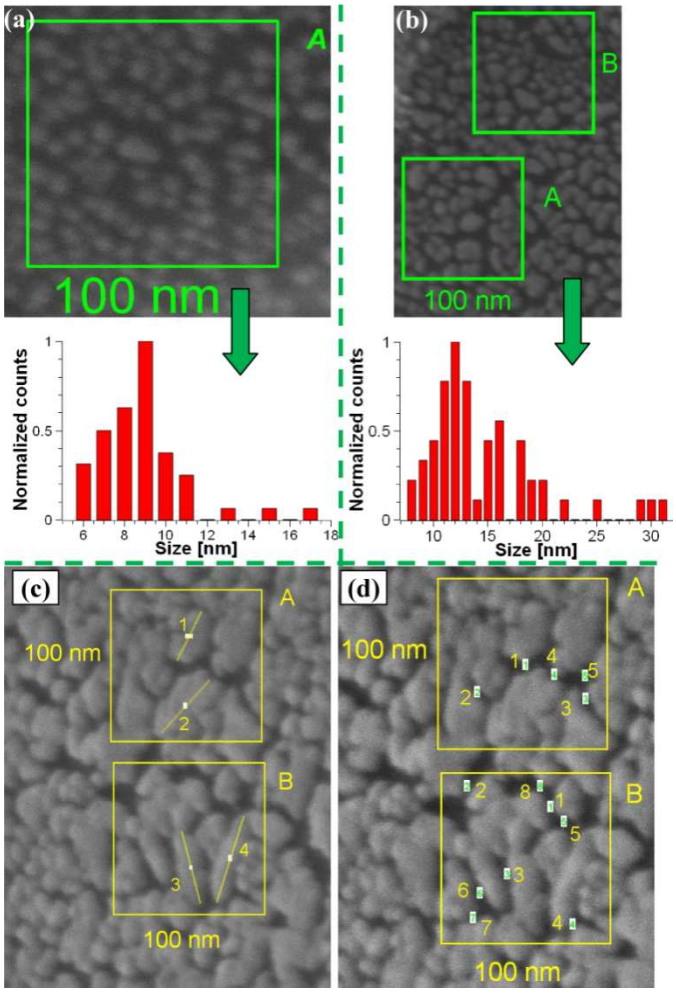

Fig. S4 (bottom- previous page) : NP size and spacing information taken at various points on the sample surface. (a) is a zoomed in inset [square is 100 nm x 100 nm] of Au NPs on an

individual GNS with a histogram showing the counts of the various sized NPs in the area indicated with a clear peak at ~9 nm, (b) presents an averaged count of the nanoparticles as marked in areas A and B [squares are 100 nm x 100 nm], (c and d) present an SEM of discontinuous Au film with a very high surface coverage - note that in Fig. S4(c) and (d) the NP size ranges between ~36 to 60 nm and spacing between ~3 to ~12 nm., labeled sizes and particle separations are listed in Table S1.

Label	Length [nm]	Label	Length [nm]
(c) A:1	35.8	(d) B:1	2.6
(c) A:2	47.0	(d) B:2	5.7
(c) B:3	48.4	(d) B:3	4.3
(c) B:4	59.5	(d) B:4	5.5
(d) A:1	7.8	(d) B:5	8.6
(d) A:2	3.2	(d) B:6	4.1
(d) A:3	4.1	(d) B:7	4.7
(d) A:4	4.3	(d) B:8	5.5
(d) A:5	11.8		

Table S1: Data from Fig. S4(c,d), to 1 d.p. accuracy, measured using ImageJ [3]

Dense Au NP patterns with small interparticle distance result in large SERS enhancements[7] which suggests that electromagnetic coupling in SERS/plasmonic applications will be more pronounced towards the center of the Au-VGNS nanoarray and less effective towards the outer edges of the Au-VGNS nanoarray,

(3) Discussion of Au nanoparticle formation and reasons for quasi-linear NP self-organization

As indicated the main text, the highest Au concentration is closest to the Au vapor source (i.e., the Au vapor travels from the filament to the GNS sample via the hole in the Cu-mesh) as expected. Upon their arrival at the surface, the Au adatoms do not have to travel very far before encountering evolving Au nanoislands whereupon they add to them, rather than nucleate new islands. The further out the Au adatom travels, the less likely it is to encounter established islands, the more likely that new (and smaller) islands will be nucleated. The situation, in this case, is a little more complicated as we are not considering diffusion on a flat multilayer graphene sample, rather we consider diffusion on vertically aligned graphene nanosheet networks. Here, Au adatom diffusion (and hence island morphology) is not only influenced by the number of graphene layers as in Zhou *et al.*[4], but also by the nature of the GNS edge termination which determines the GNS conduction mechanism and hence affects the charge exchange between the Au nanoparticles and the graphene layers.

Note that Au nanoparticles are formed through diffusion away from the point of the most gold, recall this was indicated qualitatively in Fig S1(c). This may be readily observed through SEMs, e.g in the centre of the 1 mm droplet there is an almost continuous islanded Au film, moving radially outwards leads to large, fairly close packed islands of tens of nm, further still leads to small, sparse populations with the majority of NP sizes less than 10 nm, and so on until the outer edges of the droplet are passed and there is no Au present, only GNS are observed. This is in agreement with the interpretation in the main text and is supported via the following mean field nucleation theory equations as presented by Mo *et al.*[5], namely 1) the lifetime of an adatom on the surface before it encounters an existing island:

$$\tau = 1/\sigma_S Dn$$

where σ_s is the capture number of an island of size *s*, *D* is the diffusion coefficient and *N* is the number density of islands on the surface and; 2) the nucleation rate where an adatom meets another adatom and nucleates a new island:

$$dN / d\tau = \sigma_1 D n^2$$

where σ_1 is the capture number of single adatoms and *n* is the concentration of adatoms on the surface.[5] Clearly as *N* increases, τ decreases (i.e. as more islands are closer together, an adatom will not be on the surface for a long time before it encounters an existing island which it may add to) and as *n* increases, the nucleation rate also increases (i.e. when more adatoms are closer to each other, the nucleation rate of new islands will be higher - as expected close to the Au source).

A similar argument, based on the diffusion coefficient was featured in Zhou *et al.*[4] to explain the different distribution of Au NPs on n-layer graphenes - a larger diffusion coefficient means that the adatom would cover a larger area and be more likely to encounter evolving islands and add to them, rather than nucleate new islands. This observation by Zhou *et al.* was used to infer the different surface free energies of n-layer graphenes (and consequent different surface diffusion barriers for Au adatoms) due to the quantum size effect.[4,6] As noted in the main text, the difference is that we are not considering diffusion on a flat multilayer graphene sample as in Zhou *et al.*[4] and comparable works[7,8], instead we consider vertically aligned graphene nanosheets. In this case, the emphasis is less on the variation of the layer thickness and more on the variation of the curvature and edge termination of the graphene nanosheets. Future research should thus aim at considering (1) how far the influence of the GNS edge on the Au NP morphology extends and (2) why this influence may cause the NPs to arrange themselves in a *linear* fashion, as observed in Figure 2(e-f) [main text].

On the issue of the observed quasi-linear arrangements of Au NPs on certain VGNS:

It is possible that the self-organization is influenced by the edge type of the VGNS – the presence of a Raman D-peak [in Figure 3 (a-d)] indicates that our array is likely comprised of a mixture of armchair edges, (possibly) zig-zag edges and zig-zag/armchair combined edges, hence may be a mixture of metallic and semiconducting VGNSs. It has been shown that the competition between electrostatic energy (arising from charge transfer from graphene to Au [8]) and surface tension of Au NPs on graphenes largely determines the Au NP diameter.[8] It is thus reasonable to suggest that the morphology of Au NPs on graphene nanosheets is also affected by the nature (i.e., metallic or semiconducting) and orientation (i.e., is there any curvature, any strain, etc.) of the VGNSs

(4) Calculations of typical surface coverages and 'bookshelf' coverage

By quick visual inspection it can be observed that GNS in Fig. 2(a) and (d) [main text] had close to 0 and 100 % surface coverage by gold, respectively. Using ImageJ, a 100 nm x 100 nm segment of a GNS in Fig. 2(b) was studied, the surface coverage by Au NPs was roughly estimated as 11.1% [see Fig. S5]. The method shown in Fig S6 was used to estimate a surface coverage of 84% in the case of Fig. 3(c):

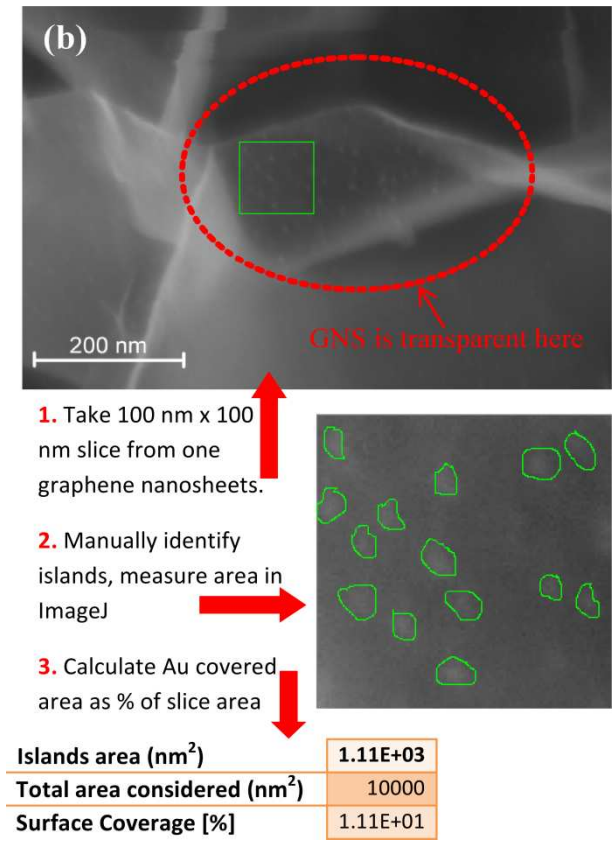

Fig. S5. How surface coverage was calculated for Fig. 2(b)

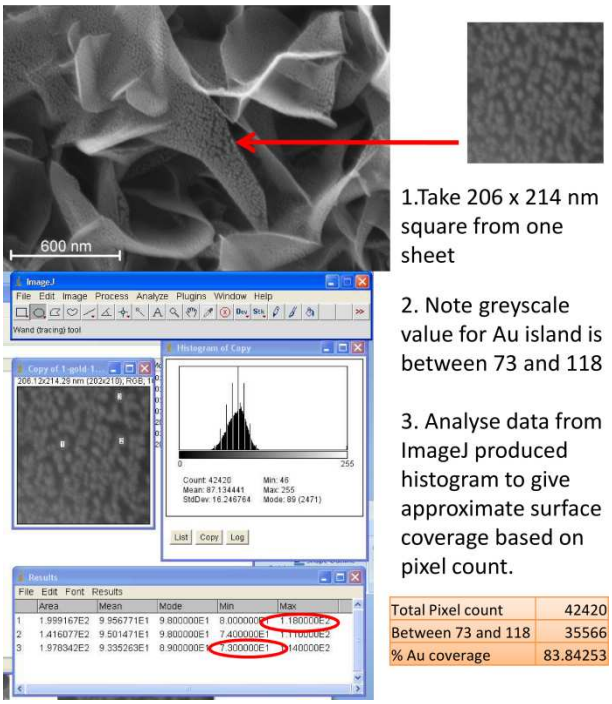

Fig. S6. How surface coverage was calculated for Fig. 2(c).

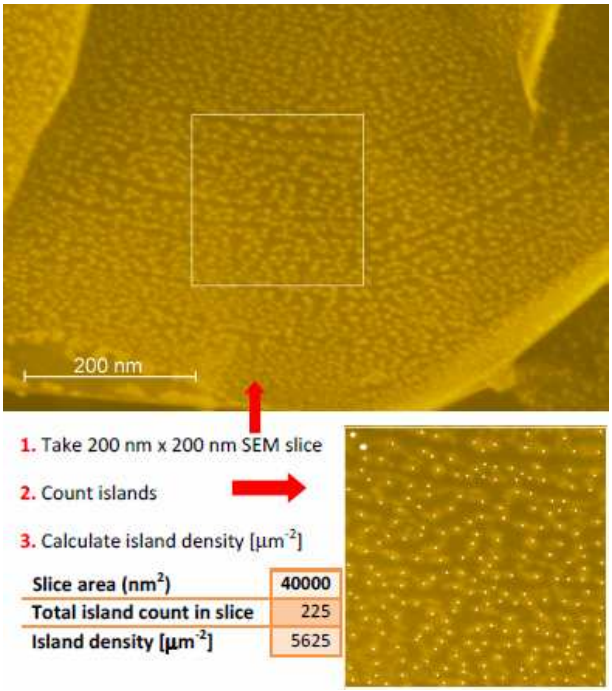

Fig. S7. How island density was calculated for Fig. 2(e).

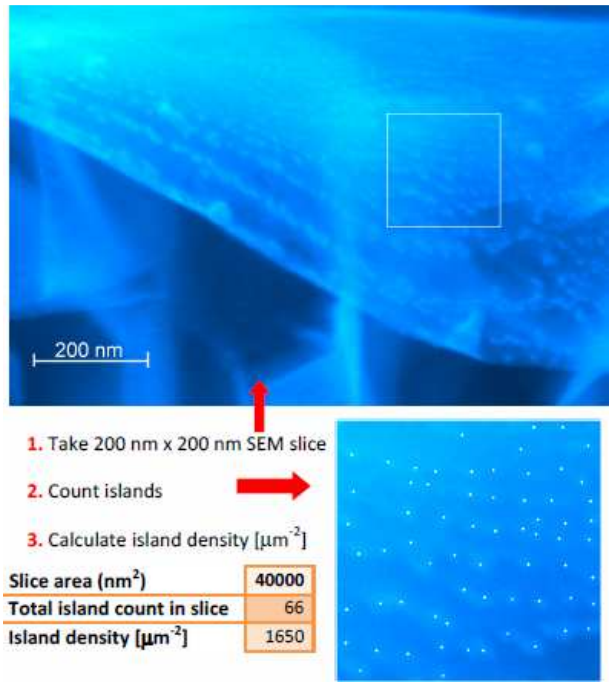

Fig. S8. How island density was calculated for Fig. 2(f)

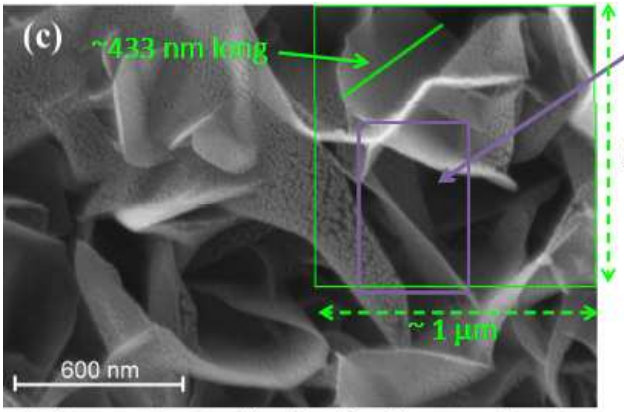

Shows Au decoration on both sides of the sheet, appears to be down to the base

Estimate of "bookshelf" density vs flat floor"

1. Conservative estimate – say 6 graphene nanosheets per 1 micron squared, approx 433 nm long & wide
2. Model GNS as rectangles – 1 sheet area = 433 x 433 nm = 187,489 nm²; times 6 → 1,124,934 nm²

3. Remembering that both sides may be decorated gives: 2,249,868 nm²
4. So we have (very conservatively) 2,249,868 nm² vs 1,000,000 nm² (1µm²)
5. Take island density per µm² as approx. 5.6 x 10^3 per 1µm² from Figure 2(e)
6. For VGNS sample – 12 faces → 5625 x 2.249868 = 12655.5075 islands
7. Consider also that the undecorated base is still available minus area the VGNS edge takes up:

$$A = 6 \times (2.8 \times 433)\ nm^2 = 7274.4\ nm^2$$

8. So: (1,000,000 – 7274.4) nm² = 992725.6 nm² → 5625 x 0.9927256 = 5584.0815 islands
9. Total island density: 12655.5075 + 5584.0815 = 18239.589 per 1µm² of 'sensor surface'
10. This is (conservatively) 324% of the value you'd get for a flat surface → an increase of 224% !!!

Fig. S9. How 'bookshelf' island density was calculated.

(5) Further discussion of the Raman spectra for Au-VGNS prior to 4-ATP immersion

From Figure 3(a-d) [main text], the ratio of the D peak intensity to the G peak intensity clearly increases with the increased surface coverage by Au nanoparticles. Also notable is the increased relative intensity of the peak at 2910 cm^{-1} (the D+G mode) with higher Au concentration as compared to the intensity of the 2D peak. In fact, for S1 the intensity of the 2910 cm^{-1} (D+G) peak is notably higher than the 2D peak (which is not the case for S2 - S4). Moreover, for S1 and S2, there is an emergence of a subtle shoulder on the left-hand side of the (D+G) peak at ~2847 cm^{-1} [see Figure 3(d)], which is clearly not present for S3 and S4. The emergence of these features may also be attributed to the amplification of the Raman modes for graphene due to the presence of the Au nanoparticles.

(6) References for Supporting Information

[1] E. E. Carpenter, A. Kumbhar, J. A. Wiemann, H. Srikanth, J. Wiggins, W. L. Zhou, C. J. O'Connor, *Mat. Sci. Eng. A.* **2000**, *286*, 81.

[2] Z. Xiong, L. L. Zhang, J. Ma, X. S. Zhao, *Chem. Commun.* **2010**, *46*, 6099.

[3] M. D. Abramoff, P. J. Magelhaes, S. J. Ram, *Biophotonics International* **2004**, *11*, 36.

[4] H. Zhou, C. Qiu, Z. Liu, H. Yang, L. Lu, J. Liu, H. Yang, C. Gu, L. Sun, *J. Am. Chem. Soc.* **2010**, *132*, 944.

[5] Y. W. Mo, J. Kleiner, M. B. Webb, M. G. Lagally, *Phys. Rev. Lett.* **1991**, 66, 1998.

[6] L-Y. Ma, L. Tang, Z-L. Guan, He K. An, X-C. Ma, J. F. Jia, Q. K. Xue, Y. Han, S. Huang, F. Liu, *Phys. Rev. Lett.* **2006**, *97*, 266102.

[7] H. Chu, J. Wang, L. Ding, D. Yuan, Y. Zhang, J. Liu, Y. Li, *J. Am. Chem. Soc.* **2009**, *131*, 14310.

[8] Z. Luo, L. A. Somers, Y. Dan, T. Ly, N. J. Kybert, E. J. Mele, A. T. C. Johnson, *Nano Lett*. **2010**,*10*,777.